Mode-locking of fiber lasers using novel two-dimensional nanomaterials: graphene and topological insulators [Invited]

Grzegorz Sobon

Laser & Fiber Electronics Group, Wroclaw University of Technology, Wybrzeze Wyspianskiego 27, 50-370 Wroclaw, Poland (grzegorz.sobon@pwr.edu.pl)

Received January 6, 2015; revised February 15, 2015; accepted February 18, 2015; posted February 18, 2015 (Doc. ID 231874); published March 26, 2015

The paper summarizes the recent achievements in the area of ultrafast fiber lasers mode-locked with so-called low-dimensional nanomaterials: graphene, topological insulators (Bi_2Te_3, Bi_2Se_3, Sb_2Te_3), and transition metal sulfide semiconductors, like molybdenum disulfide (MoS_2). The most important experimental achievements are described and compared. Additionally, new original results on ultrashort pulse generation at 1.94 μm wavelength using graphene are presented. The designed Tm-doped fiber laser utilizes multilayer graphene as a saturable absorber and generates 654 fs pulses at 1940 nm wavelength, which are currently the shortest pulses generated from a Tm-doped fiber laser with a graphene-based saturable absorber.

OCIS codes: (140.4050) Mode-locked lasers; (140.3510) Lasers, fiber; (060.3510) Lasers, fiber.
http://dx.doi.org/10.1364/PRJ.3.000A56

1. INTRODUCTION

Ultrashort pulsed sources of optical radiation in the infrared range are currently on demand for many industrial, military, and medical applications, such as laser micromachining [1], surgery [2], terahertz-wave generation [3], optical imaging [4], or supercontinuum generation [5]. Fiber lasers, thanks to their compactness, cost-effectiveness, and robustness, are excellent candidates for this type of application. In order to force a fiber laser to generate ultrashort pulses, it is necessary to synchronize the phases of the longitudinal modes in the resonator. This might be done in two ways: by placing a saturable absorber (SA) device inside the cavity or by taking advantage of nonlinear effects occurring in optical fibers: nonlinear polarization rotation (NPR) [6,7] or nonlinear amplification loop mirror (the so-called figure-8 configuration [8]). The currently most common and popular SA—semiconductor SA mirror (SESAM), widely used in commercially available systems—is based on quantum wells in semiconductors [9]. It has a very rich, 20-year history and is still developed, especially for thin-disk lasers [10]. However, SESAMs suffer from relatively narrowband operation—due to the energy bandgap in semiconductors, each SESAM needs to be designed for a specific wavelength. Thus, it is not possible to mode-lock lasers operating in different wavelength bands or to synchronize two oscillators using one common SA. Figure-8 and NPR-based lasers tend to be environmentally unstable, are vulnerable to fiber movement, and do not always provide self-starting pulsed operation. All those drawbacks forced the ultrafast laser community to search for new types of SAs, based on novel materials.

In the recent five years, so called two-dimensional (2D) nanomaterials revolutionized the field of mode-locked lasers. A 2D material is often defined as an atomically thin layered material, and its thickness is reduced down to single or only a few layers [11–13]. In such a material, strong intralayer covalent bonding and weak interlayer van der Waals forces are present [14]. In the absence of interlayer perturbation, the electron motion is limited to two dimensions [15], which may lead to many new and unexpected electronic and optical properties. The most popular example of a 2D material is graphene, which is composed of a one-atom-thick layer of carbon forming a 2D honeycomb lattice. Graphene is a fundamental building block of three-dimensional (3D) graphite. Other 2D materials usable in laser technology include topological insulators (TIs; Bi_2Te_3, Bi_2Se_3, Sb_2Te_3) and transition metal sulfide semiconductors, like molybdenum disulfide (MoS_2). The growing interest in novel 2D materials started in 2009, when the groups from Singapore and United Kingdom independently developed the first graphene-based fiber lasers [16,17]. In the next five years, hundreds of new laser setups were reported in the literature, utilizing not only graphene but also TIs and recently transition metal sulfides. The field of fiber lasers has experienced an unprecedented and very fast progress, leading to many outstanding achievements.

In this paper, the most important recent achievements in the field of fiber lasers incorporating 2D materials are summarized. Additionally, original results on ultrashort pulse generation at 1.9 μm using multilayer graphene are presented.

2. SATURABLE ABSORBERS BASED ON 2D NANOMATERIALS

2D nanomaterials are currently intensively investigated among the applied physics and photonics community. The most important materials that might be used as SAs for mode-locked fiber lasers include carbon nanotubes (CNTs), graphene, TIs (Bi_2Te_3, Bi_2Se_3, Sb_2Te_3), and transition metal sulfide semiconductors such as MoS_2 or tungsten disulfide

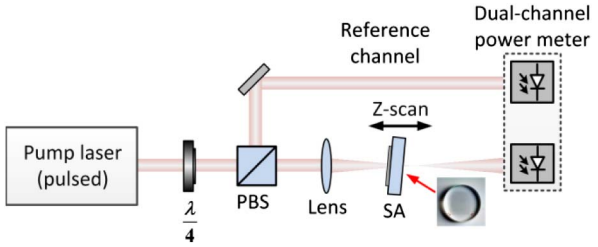

Fig. 1. Z-scan setup for power-dependent transmission measurement of free-space SA.

(WS_2) [18]. Mode-locking of fiber lasers using all those materials has been already reported in the literature. A typical SA is characterized by three basic parameters: modulation depth (α_0), saturation intensity (I_{sat}), and nonsaturable losses (α_{NS}). All those parameters are bound with a simple formula, which describes the power-dependent absorption $\alpha(I)$ of a SA [19]:

$$\alpha(I) = \frac{\alpha_0}{1 + \frac{I}{I_{\text{sat}}}} + \alpha_{\text{NS}}. \quad (1)$$

The parameters of SAs operating as transmission devices (not reflecting, that is, SESAMs) might be measured in two ways. For free-space coupled absorbers (e.g., graphene deposited on a glass window) a typical Z-scan setup might be used. It is schematically drawn in Fig. 1. A pulsed laser (femto- or picosecond) is used as a pumping source. The pumping light is divided into two beams: the reference and the measurement beam. Usually the greater part of the power is directed to the SA. The sample is moved in the z-axis along the waist of the beam, which changes the light intensity per unit area. The dual-channel power meter measures the power in both arms.

For fiber-based devices (e.g., graphene deposited on a fiber connector) the typical measurement setup looks like that depicted in Fig. 2. Again, a femtosecond/picosecond laser is used as pumping source. However, here the setup is fully fiberized. The power is changed using a variable optical attenuator. A typical fiber coupler splits the power between the reference and measurement arm. Again, the greater part of the power traverses through the SA. At the end, the power in both arms is measured by the dual-channel power meter.

There are several techniques of fabricating SAs based on nanomaterials and making them suitable for use in a fiber laser. The most popular approaches are schematically explained in Fig. 3. The material might be deposited on glass plates [Fig. 3(a)], on a fiber connector end facet [Fig. 3(b)], on a tapered optical fiber [Fig. 3(c)], or on the surface of a side-polished fiber [Fig. 3(d)].

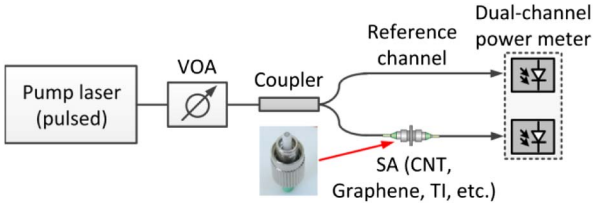

Fig. 2. Typical setup for power-dependent transmission measurement of fiber-based SAs.

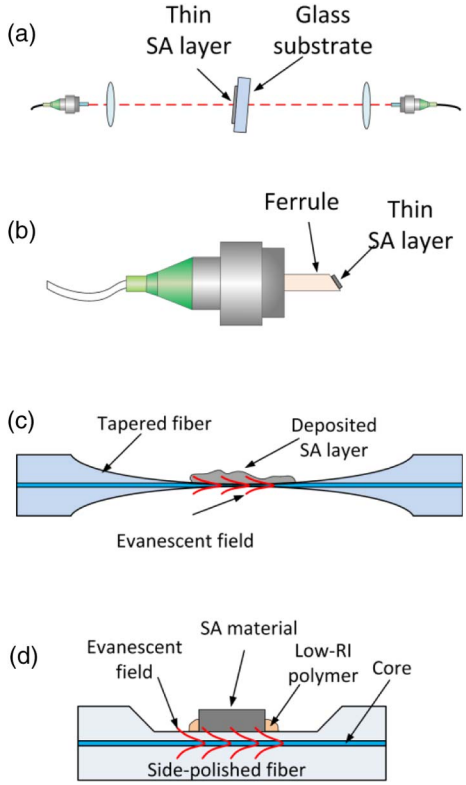

Fig. 3. Different types of SAs based on nanomaterials: (a) deposited on a glass plate, (b) on a fiber connector tip, (c) on a tapered fiber, and (d) on a side-polished fiber (RI—refractive index).

3. TOPOLOGICAL INSULATORS AS SATURABLE ABSORBERS FOR FIBER LASERS

A TI is a material which is characterized by an insulating bulk state and a Dirac-type surface state. The existence of this new state of quantum matter was predicted theoretically in 2005 [20] and verified experimentally in 2007, when surface metallic states were observed in HgTe/CdTe quantum wells broader than 6.5 nm [21]. Up till now, tens of different TIs were identified [22]. Due to their graphene-like energy bandgap structure with characteristic Dirac cones, TIs (which were up till now investigated) exhibit a very broad and relatively flat light absorption [23]. Three of them have found very much attention in the photonics community: Bi_2Te_3, Bi_2Se_3, and Sb_2Te_3. For those materials, the carrier recombination mechanism was already investigated [23–26], using time-resolved and angle-resolved photoelectron spectroscopy.

The first ultrafast fiber laser incorporating a TI was demonstrated in 2012 by Zhao *et al.* [27]. The laser was incorporating a Bi_2Te_3-based SA and emitted 1.21 ps pulses at 1558 nm. The measurements also revealed a very high modulation depth of the used TI and broad, flat absorption in the range of 1000 to 1800 nm [27]. Further studies on the third-order nonlinear properties of Bi_2Te_3 performed by the same group revealed that the material might exhibit modulation depth up to 61.2% and possesses a very high third-order nonlinear refractive index, at the level of 10^{-14} m^2/W [28]. After the first demonstration, a number of reports on TI-based fiber lasers appeared. The most prominent and important include: the first demonstration of a Bi_2Se_3-based fiber laser [29], the first

demonstration of harmonic mode-locking with Bi_2Te_3 [30], first demonstration of the usage of Sb_2Te_3 TI for mode-locking [31], harmonic mode-locking with Sb_2Te_3 [32], development of TI-polymer composites [33], and many others.

High quality TI films can be obtained by molecular beam epitaxy growth [34], vapor-liquid-solid growth [35], mechanical exfoliation of thin sheets from bulk crystals [36], or liquid phase exfoliation (LPE), forming solutions with TI sheets dispersed in solvents, like acetone or isopropyl alcohol [27,29] or polymers, like polyvinyl alcohol (PVA) [33].

The historically first Er-doped fiber lasers based on Bi_2Te_3 and Bi_2Se_3 incorporated a quartz plate with deposited thin TI layer (droplet of a TI liquid solution and dried) [27,29]. Such a plate was inserted into the cavity as a free-space SA, as depicted in Fig. 3(a). In both reports the absorbers were characterized by almost 98% of modulation depth. They supported generation of 1.21 ps-short solitons at 1558 nm [27], and also solitons tunable from 1557 to 1565 nm with 1.57 ps duration [29]. Probably the most popular approach is to deposit a thin TI layer on the end facet of a fiber connector [31,33,37]. This method is also widely used with other SA materials, like CNTs and graphene. The material might be either mechanically exfoliated [31] or deposited from liquid phase and dried [33]. Liu *et al.* [33] reported fabrication of a Bi_2Se_3-PVA composite, which was next placed on a fiber connector tip. The TI-PVA SA exhibited modulation depth at the level of 3.9% and saturation intensity of 12 MW/cm^2, and supported mode-locking with 690 fs pulses at 1557 nm [33]. In [37] the authors report a mechanically exfoliated Bi_2Te_3 SA with 3% of modulation depth, which supported generation of 403 fs pulses. In 2013, Sotor *et al.* [31] demonstrated, for the first time, the usage of Sb_2Te_3 TI as SA for mode-locking. The developed laser was capable of generating 1.8 ps-short pulses at repetition rate of 4.75 MHz.

Recently, an evanescent field interaction technique was also applied to TIs. In this approach, the material is deposited either on a tapered fiber or on a side-polished fiber [Figs. 3(c) and 3(d)]. The saturable absorption is based on the interaction between the material and the evanescent field propagating in the cladding of the fiber. This approach seems to be more robust and reliable in comparison to end-face deposition because of a higher damage threshold [38,39]. This technique led already to many impressive results. As an example, Lee *et al.* demonstrated an Er-doped fiber laser emitting 600 fs pulses with a SA based on a bulk structured Bi_2Te_3 placed on a side-polished (D-shaped) fiber [40]. The same group of authors reported 795 fs pulse generation at 1935 nm from a Tm/Ho-doped fiber laser using a similar SA for mode-locking, but with slightly larger modulation depth (20%) [41]. Instead of a bulk material, also TI-dispersions might be used to cover a side-polished fiber or a tapered fiber. Recently, Boguslawski *et al.* demonstrated a SA based on LPE Sb_2Te_3, dispersed in chitosan solution, deposited on a side-polished fiber. The Er-doped fiber laser emitted 449 fs pulses at 22 MHz repetition rate [42]. In order to take advantage from the evanescent field propagating in the cladding, also microfibers (tapered fibers) might be used. As an example, Luo *et al.* [30] developed a fiber which was tapered down to 12 μm and covered with Bi_2Te_3 nanosheets dispersed in acetone solution. The modulation depth of the SA was relatively low (at the level of 1.7%); thus the laser favored a harmonic mode-locking regime. In the experiment, a repetition rate of 2 GHz could be achieved. The same group of authors also used a similar SA for dual-wavelength mode-locking of an Er-doped fiber laser [43].

Up till now, the shortest pulse ever generated from a fiber laser incorporating a TI is 128 fs and was achieved from a dispersion-managed Er-doped fiber laser with Sb_2Te_3 [39]. The SA was based on a side-polished (D-shaped) optical fiber. A bulk piece of Sb_2Te_3 was placed on the polished region with the presence of low-refractive-index polymer. In this case, there was no need to exfoliate the material and achieve thin layers, because the evanescent field interacts only with the surface of the bulk crystal. Such a prepared SA exhibits a modulation depth at the level of 6%, with nonsaturable losses at the level of 43% and saturation intensity of 31 MW/cm^2. Those parameters make this device suitable for mode-locking in an Er-doped fiber laser. The laser generated a very broad spectrum (almost 70 nm considering a 10 dB bandwidth) and output pulses at the level of 128 fs after dechirping.

The method of depositing a bulk piece of material on a side-polished fiber presented in [39] also enables observation of other mode-locking regimes, depending on the cavity dispersion. Besides stretched-pulse operation, also solitons (in all-anomalous dispersion) and dissipative solitons (all-normal dispersion) might be observed [44,45]. The parameters of all fundamentally mode-locked fiber lasers with TI-based SAs are summarized in Table 1.

4. TRANSITION METAL SULFIDES AS SATURABLE ABSORBERS

The group of transition metal dichalcogenides (TMDCs) contains about 60 different compounds, and about 60% of them are characterized by a layered structure [46]. Those materials were already investigated very strongly in the late 1960s [47]. The rapid growth of graphene science has renewed the general interest in TMDCs. Materials as such as MoS_2, $MoSe_2$, WS_2, and WSe_2 have found great interest in the applied physics community, since they allow applications as transistors, photodetectors, and optoelectronic devices [48]. Mode-locking in fiber lasers using one of the TMDCs, namely MoS_2, is unquestionably one of the most important recent achievements in laser technology. This material is characterized by a layered structure, similar to that in graphite/graphene. Thus, it can be even mechanically exfoliated to obtain single layers. Nonlinear optical properties, like saturable absorption and nonlinear refractive index, in MoS_2 nanosheets were investigated in 2013 [14]. The experiments performed by Wang *et al.* have revealed that a MoS_2 dispersion might change its transmission by about 10% under high-intensity pulsed excitation. Less than one year after that discovery, the first application of MoS_2 as a SA was presented by Zhang *et al.* [15]. The presented Yb-doped fiber laser was mode-locked with MoS_2 nanosheets dispersed via LPE and deposited on a fiber connector. Due to the all-normal cavity design, the laser generated chirped dissipative solitons with 2.7 nm FWHM at 1054 nm central wavelength. The same group of authors has demonstrated femtosecond pulse generation from an Er-doped fiber laser mode-locked with a PVA-based MoS_2 SA [49]. The laser generated 710 fs pulses centered at 1569.5 nm wavelength with a repetition rate of 12.09 MHz. Wavelength-tunable operation of a MoS_2-based fiber laser

Table 1. Summary of the Reported Fundamentally Mode-Locked Fiber Lasers with TI-Based SAs

Reference	SA	λ_{center} [nm]	$\Delta\lambda_{FWHM}$ [nm]	τ_{pulse} [fs]
Zhao *et al.* [27]	Free-space coupled, Bi_2Te_3 on quartz (LPE)	1558	2.69	1210
Zhao *et al.* [29]	Free-space coupled, Bi_2Se_3 on quartz (LPE)	1564	1.79	1570
Luo *et al.* [30]	Bi_2Te_3 (LPE in acetone) on microfiber	1558	0.95	1220
Lee *et al.* [40]	Bulk Bi_2Te_3 deposited on D-shaped fiber	1547	4.63	600
Jung *et al.* [41]	Bulk Bi_2Te_3 deposited on D-shaped fiber	1935	5.6	795
Liu *et al.* [33]	Bi_2Se_3/PVA composite on fiber connector	1557	4.3	660
Lin *et al.* [37]	Mech. exfoliated Bi_2Te_3 on fiber connector	1570	6.86	403
Sotor *et al.* [31]	Mech. exfoliated Sb_2Te_3 on fiber connector	1558	1.8	1800
Sotor *et al.* [39]	Bulk Sb_2Te_3 deposited on D-shaped fiber	1565	30	128
Boguslawski *et al.* [42]	Sb_2Te_3 (LPE) on D-shaped fiber	1556	6	449
Sotor *et al.* [44]	Bulk Sb_2Te_3 deposited on D-shaped fiber	1561	10.3	270
Sotor *et al.* [32]	Mech. exfoliated Sb_2Te_3 on fiber connector	1558	1.59	1900
Liu *et al.* [43]	Bi_2Te_3 (LPE in acetone) on microfiber	1558	0.9	3010

in a very broad spectral range was reported by Zhang *et al.* [50]. The demonstrated laser utilized a PVA-MoS_2 SA and enabled continuous tuning from 1535 to 1565 nm. Those experiments prove wideband operation of MoS_2 as SA. MoS_2 is also suitable for use in combination with tapered fibers (microfibers). Du *et al.* demonstrated an Yb-doped fiber laser which generated dissipative solitons at 1042.6 nm with pulse duration of 656 ps and a repetition rate of 6.74 MHz [51]. Recently, also harmonic mode-locking at 1.56 μm was demonstrated in a fiber laser incorporating a microfiber-based MoS_2 SA [52]. Repetition rates up to 2.5 GHz (corresponding to the 369th harmonic of the fundamental mode spacing) could be achieved. Summarizing, MoS_2 SAs have proven their usability for mode-locking of fiber lasers operating at different wavelengths from 1 to 1.56 μm, including harmonic mode-locking, dissipative soliton generation, and continuously tunable operation. It can be predicted that in the next years MoS_2-based devices will exhibit comparable performance to graphene- or TI-based SAs.

5. GRAPHENE-BASED FIBER LASERS

Graphene gained such huge interest from scientists working in the field of ultrafast lasers due to its unique optical properties. The pump-probe measurements revealed that graphene is characterized by a fast relaxation transient in the 70–150 fs range, followed by a slower relaxation process in the 0.5–2.0 ps range [53,54]. The saturable absorption properties of graphene were also measured using the techniques described in Section 2. Typically, a single layer of graphene absorbs 2.3% of incident low-intensity light in a very broad spectrum of wavelengths [55]. Some part of this absorption might be saturated when the incident intensity is increased. However, the modulation depth of graphene is wavelength-dependent and has typical values between 0.5% and 1.8% per layer. Table 2 summarizes the parameters of monolayer graphene measured at different wavelengths: the modulation depth (ΔT), nonsaturable losses (α_{NS}), saturation fluence (F_{sat}), and the slow relaxation time (τ_R).

Table 2. Summary of the Reported Saturable Absorption Parameters of Monolayer Graphene

λ [nm]	τ_R [ps]	ΔT [%]	α_{NS} [%]	F_{sat}[μJ/cm^2]	Ref.
800	1.47	1.8	< 0.9	66.5	[56]
1040	1.5	0.75	1.59	50	[57]
1250	1.45	0.54	1.61	14.5	[58]
1500	1.5	0.5	1.9	14	[59]

Such low modulation depth at wavelengths around 1.5 μm is not always sufficient to start mode-locking in a fiber laser. Thus, it is usually necessary to increase the number of layers, which results in increased modulation depth and nonsaturable losses. Most of the actual state-of-art graphene-based lasers operate using multilayer graphene [60–62].

Graphene suitable for mode-locking of fiber lasers might be produced using several methods. The most common include: epitaxial growth via chemical vapor deposition (CVD), LPE, and mechanical exfoliation. The CVD technique allows obtaining high quality graphene with a precisely controlled number of layers, starting from monolayer (grown on SiC [63] or Cu substrates [64]) up to multilayer (on Ni foils [65,66]). Graphene might be afterwards transferred onto mirrors [67], glass windows [68], or fiber connectors [69] with the use of polymer support, such as poly(methyl methacrylate) (PMMA), and serve as a mode-locker.

The most popular and common technology of fabricating a graphene-based SA is based on fiber connectors [Fig. 3(b)]. For this purpose, LPE graphene is mainly used. Chemical functionalization offers a variety of solvents, in which the graphene flakes may be dispersed, such as dimethylformamide (DMF) [70]. Such solutions can be afterwards mixed with polymers, forming stable and thin composites which also may be deposited on fiber connectors [60,62]. Recently, a new solvent for graphene has been proposed, namely chitosan [71]. The main advantage of chitosan, in contrast to many other available solvents, is biocompatibility and atoxicity. It might be used as an exfoliating and stabilizing compound. Safety of usage and relatively low cost make chitosan an interesting material for photonics applications. Long chains of chitosan enable separating graphene layers and prevent them from reagglomeration after exfoliation of graphite. This polysaccharide is stable under the operating conditions of fiber lasers and provides good distribution of the sheets on the fiber surface. The usage of a graphene/chitosan composite allows us to obtain the shortest pulses ever generated from a fiber laser incorporating a graphene SA: 168 fs from an Er-doped fiber laser at 1555 nm [71].

The main and undisputed advantage of graphene over other narrowband SAs, like SESAM, is its extremely broad operation bandwidth. This unique property of graphene might lead to many novel concepts, like dual-band fiber lasers,

Table 3. Summary of the Reported TDFLs with Graphene SA

Reference	SA Type	λ_{center} [nm]	$\Delta\lambda_{FWHM}$ [nm]	τ_{pulse} [ps]	f_{rep} [MHz]	P_{out} [mW]
Zhang *et al.* [76]	LPE (PVA)	1942	2.1	3.6	6.46	2
Wang *et al.* [77]	LPE (DMF)	1953	2.2	2.1	16.94	1.41
Sobon *et al.* [78]	CVD (PMMA)	1884	4	1.2	20.5	1.35

mode-locked with one common SA. In [72] Sotor *et al.* demonstrated an all-fiber Tm- and Er-doped fiber laser, simultaneously mode-locked with one common SA, that generated ultrashort pulses at wavelengths separated by almost 400 nm. The laser consisted of two ring resonators with one common branch, containing also the graphene-based SA. The laser generated optical solitons at 1565 and 1944 nm. This was the first experimental confirmation of the broadband saturable absorption property of graphene. This achievement led to another interesting experiment, where both loops were passively synchronized [73]. The graphene-SA supported simultaneous generation of synchronized ultrashort pulses at 1558 and 1938 nm with 67 fs of RMS timing jitter. It was also confirmed that the nonlinearities of graphene enhance the possibility of passive synchronization of both lasers, extending the synchronization holding range by 85% [73].

A. Graphene-Based Tm-Doped Fiber Lasers

Fiber lasers operating in the 2 μm spectral region are currently one of the most important branches of laser technology. They are experiencing intense development due to their importance in many scientific applications, such as remote sensing, spectroscopy, and medicine. The 1.8–2.0 μm spectral range, covered by thulium-doped fiber lasers (TDFLs), overlaps with absorption lines of several molecules, such as carbon dioxide (CO_2) or hydrogen bromide (HBr), which creates the possibility of constructing cost-effective trace-gas sensing platforms [74]. Strong water absorption in this range makes TDFLs extremely desirable in biomedical applications. Due to strong absorption in water (which is the main constituent of the human body), heating of only small areas is achieved. The light penetration into the tissue is at the level of micrometers, which allows precise cutting of biological tissue. Additionally, bleeding is suppressed by coagulation [75].

Interestingly, to date there have been only three reports on TDFLs incorporating a graphene-based SA. The first demonstration was done by Zhang *et al.* in 2012 [76]. The authors have achieved 3.6 ps pulses at 1.94 μm using chemically exfoliated graphene (via the LPE method) dispersed in a PVA host. Later, Wang *et al.* demonstrated a TDFL emitting 2.1 ps pulses [77]. This laser was also utilizing graphene exfoliated by an ultrasonic method; however, in this case the layers were dispersed in DMF. In 2013 our group reported an all-fiber TDFL which generated 1.2 ps pulses at 1884 nm, using a CVD-graphene/PMMA composite [78]. Table 3 summarizes the recent achievements in Tm-doped graphene-based lasers.

The CVD method of obtaining graphene layers is very convenient for laser applications, since it allows scaling the number of graphene layers on one substrate [65]. Stacking of graphene layers on one PMMA supporting layer allows scaling the modulation depth and nonsaturable losses of the SA and might lead to very interesting results. Figure 4 shows the experimental setup of a TDFL based on a CVD-graphene/PMMA SA. The resonator consists of a 10 cm piece of

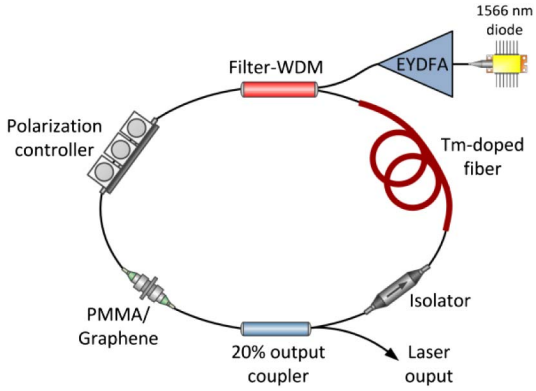

Fig. 4. Experimental setup of the TDFL with CVD-graphene/PMMA SA.

Tm-doped fiber (Nufern SM-TSF-5/125) with high dopant concentration, a filter-type wavelength division multiplexer for 1570/2000 nm wavelengths, an isolator, a polarization controller, a 20% output coupler, and the SA. The laser was pumped by a 1566 nm laser diode, amplified in an erbium–ytterbium co-doped fiber amplifier (EYDFA) to about 340 mW. The length of the cavity was around 5.3 m, resulting in a repetition frequency equal to 38.45 MHz.

As a SA, we have used a stack of 21 graphene layers immersed in a PMMA supporting layer. A piece of graphene/PMMA foil was deposited on the end facet of a fiber connector [as shown in Fig. 3(b)]. Such SA exhibits 5.5% of modulation depth with less than 31% of nonsaturable losses. Figure 5 shows the measured power-dependent transmission curve in a setup like that presented in Fig. 2, together with a theoretical fit calculated from Eq. (1). It can be seen, that the saturation fluence of the SA [I_{sat} in Eq. (1)], defined as the half value of the modulation depth, is around 100 μJ/cm^2.

Figure 6 shows the recorded optical spectrum generated by the laser. It has a typical soliton-like shape with visible

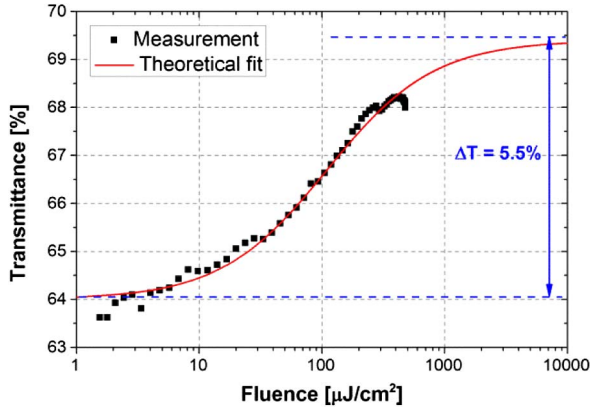

Fig. 5. Measured power-dependent transmission of the 21-layer graphene (dotted line) together with the theoretical fit (solid red line).

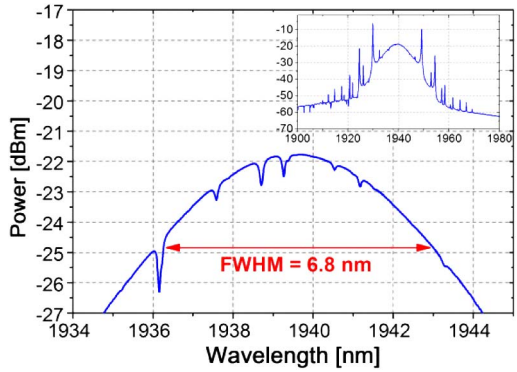

Fig. 6. Optical spectrum generated by the TDFL.

Kelly's sidebands. The central wavelength of the emission is 1939.6 nm with 6.8 nm of FWHM bandwidth. Several dips present on the optical spectrum are caused by strong water absorption in that spectral region.

Figure 7 depicts the measured radio-frequency (RF) spectrum of the laser output. The repetition frequency is equal to 38.45 MHz, corresponding to a 5.3 m long cavity. The signal to noise ratio is larger than 77 dB (measured at resolution bandwidth of 33 Hz), which is very satisfactory and much better than in previously reported graphene-based 2 μm lasers [76,77]. The RF spectrum in the full available span (3 GHz) is shown inset Fig. 7. It shows a broad spectrum of harmonics, indicating that the laser works stably.

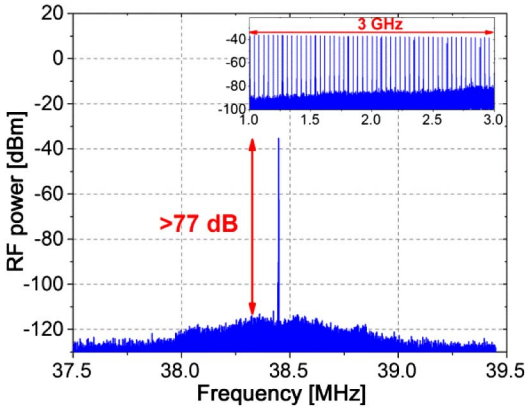

Fig. 7. Measured RF spectrum of the TDFL.

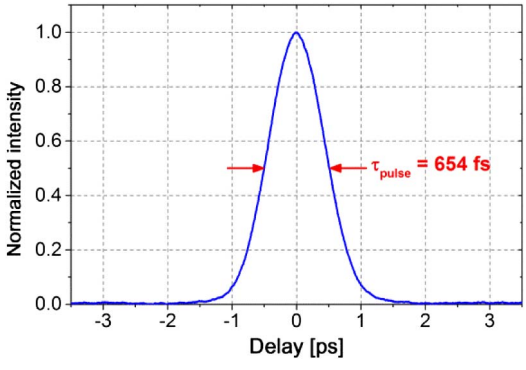

Fig. 8. Autocorrelation trace of the 654 fs pulse generated from the mode-locked TDFL.

The laser generates 654 fs pulses (assuming a sech^2 shape, typical for soliton lasers in the all-anomalous dispersion regime). The measured autocorrelation trace is depicted in Fig. 8. The time-bandwidth product of the laser is equal to 0.354, which means that the pulses are slightly chirped and might be shortened closer to the transform-limited value of 581 fs by compensating the dispersion at the laser output. The 654 fs pulses are currently the shortest pulses ever generated from a graphene-based, TDFL, almost two times shorter than the actual record (1.2 ps in [78]).

6. SUMMARY

In conclusion, the recent most important advances in the field of ultrafast lasers utilizing 2D materials has been summarized. We can definitely say that 2D materials like graphene, TIs, and transition metal sulfides have revolutionized the field of mode-locked lasers. They constitute a low-cost and robust alternative to semiconductor-based and artificial SAs. The discovery of unique optical properties of 2D nanomaterials has initiated an extremely fast progress in the field of fiber lasers, which definitely will not slow down in the next years, thanks to the ongoing research on novel nanomaterials.

ACKNOWLEDGMENTS

The experimental research presented in this paper was supported by the National Science Centre (NCN, Poland) under the research project entitled "Passive mode-locking in dispersion-managed ultrafast thulium-doped fiber lasers" (decision no. DEC-2013/11/D/ST7/03138). The author expresses his thanks to the members of the Laser & Fiber Electronics Group (Dr. Jaroslaw Sotor, Jan Tarka, Jakub Boguslawski, and Prof. Krzysztof Abramski) for their help and valuable discussions.

REFERENCES

1. R. R. Gattass and E. Mazur, "Femtosecond laser micromachining in transparent materials," Nat. Photonics **2**, 219–225 (2008).
2. N. Mamalis, "Femtosecond laser: the future of cataract surgery?" J. Cataract Refract. Surg. **37**, 1177–1178 (2011).
3. D. Stehr, C. M. Morris, C. Schmidt, and M. S. Sherwin, "High-performance fiber-laser-based terahertz spectrometer," Opt. Lett. **35**, 3799–3801 (2010).
4. S. Tang, J. Liu, T. B. Krasieva, Z. Chen, and B. J. Tromberg, "Developing compact multiphoton systems using femtosecond fiber lasers," J. Biomed. Opt. **14**, 030508 (2009).
5. G. Sobon, M. Klimczak, J. Sotor, K. Krzempek, D. Pysz, R. Stepien, T. Martynkien, K. M. Abramski, and R. Buczynski, "Infrared supercontinuum generation in soft-glass photonic crystal fibers pumped at 1560 nm," Opt. Mater. Express **4**, 7–15 (2014).
6. K. Krzempek, G. Sobon, P. Kaczmarek, and K. M. Abramski, "A sub-100 fs stretched-pulse 205 MHz repetition rate passively mode-locked Er-doped all-fiber laser," Laser Phys. Lett. **10**, 105103 (2013).
7. A. Komarov, H. Leblond, and F. Sanchez, "Passive harmonic mode-locking in a fiber laser with nonlinear polarization rotation," Opt. Commun. **267**, 162–169 (2006).
8. I. N. Duling, "All-fiber ring soliton laser mode locked with a nonlinear mirror," Opt. Lett. **16**, 539–541 (1991).
9. U. Keller, K. J. Weingarten, F. X. Kärtner, D. Kopf, B. Braun, I. D. Jung, R. Fluck, C. Hönninger, N. Matuschek, and J. Aus der Au, "Semiconductor saturable absorber mirrors (SESAMs) for femtosecond to nanosecond pulse generation in solid-state lasers," IEEE J. Sel. Top. Quantum Electron. **2**, 435–453 (1996).
10. C. Schriber, F. Emaury, A. Diebold, S. Link, M. Golling, K. Beil, C. Kränkel, C. J. Saraceno, T. Südmeyer, and U. Keller,

"Dual-gain SESAM modelocked thin disk laser based on Yb: Lu_2O_3 and Yb:Sc_2O_3," Opt. Express **22**, 18979–18986 (2014).
11. M. Xu, T. Liang, M. Shi, and H. Chen, "Graphene-like two-dimensional materials," Chem. Rev. **113**, 3766–3798 (2013).
12. A. H. C. Neto and K. Novoselov, "Two-dimensional crystals: beyond graphene," Mater. Express **1**, 10–17 (2011).
13. C. Janisch, N. Mehta, D. Ma, A. L. Elías, N. Perea-López, M. Terrones, and Z. Liu, "Ultrashort optical pulse characterization using WS_2 monolayers," Opt. Lett. **39**, 383–385 (2014).
14. K. Wang, J. Wang, J. Fan, M. Lotya, A. O'Neill, D. Fox, Y. Feng, X. Zhang, B. Jiang, Q. Zhao, H. Zhang, J. N. Coleman, L. Zhang, and W. J. Blau, "Ultrafast saturable absorption of two-dimensional MoS_2 nanosheets," ACS Nano **7**, 9260–9267 (2013).
15. H. Zhang, S. B. Lu, J. Zheng, J. Du, S. C. Wen, D. Y. Tang, and K. P. Loh, "Molybdenum disulfide (MoS_2) as a broadband saturable absorber for ultra-fast photonics," Opt. Express **22**, 7249–7260 (2014).
16. Q. L. Bao, H. Zhang, Y. Wang, Z. H. Ni, Z. X. Shen, K. P. Loh, and D. Y. Tang, "Atomic layer graphene as saturable absorber for ultrafast pulsed laser," Adv. Funct. Mater. **19**, 3077–3083 (2009).
17. T. Hasan, Z. Sun, F. Wang, F. Bonaccorso, P. H. Tan, A. G. Rozhin, and A. C. Ferrari, "Nanotube–polymer composites for ultrafast photonics," Adv. Mater. **21**, 3874–3899 (2009).
18. K. Wu, X. Zhang, J. Wang, X. Li, and J. Chen, "WS_2 as a saturable absorber for ultrafast photonic applications of mode-locked and *Q*-switched lasers," arXiv:1411.5777v1 (2014).
19. F. X. Kärtner, J. Aus der Au, and U. Keller, "Mode-locking with slow and fast saturable absorbers—what's the difference?" IEEE J. Sel. Top. Quantum Electron. **4**, 159–168 (1998).
20. C. L. Kane and E. J. Mele, "Z2 topological order and the quantum spin hall effect," Phys. Rev. Lett. **95**, 146802 (2005).
21. M. König, S. Wiedmann, C. Brüne, A. Roth, H. Buhmann, L. W. Molenkamp, X.-L. Qi, and S.-C. Zhang, "Quantum spin hall insulator state in HgTe quantum wells," Science **318**, 766–770 (2007).
22. Y. Ando, "Topological insulator materials," J. Phys. Soc. Jpn. **82**, 102001 (2013).
23. H. Peng, W. Dang, J. Cao, Y. Chen, D. Wu, W. Zheng, H. Li, Z.-X. Shen, and Z. Liu, "Topological insulator nanostructures for near-infrared transparent flexible electrodes," Nat. Chem. **4**, 281–286 (2012).
24. M. Hajlaoui, E. Papalazarou, J. Mauchain, G. Lantz, N. Moisan, D. Boschetto, Z. Jiang, I. Miotkowski, Y. P. Chen, A. Taleb-Ibrahimi, L. Perfetti, and M. Marsi, "Ultrafast surface carrier dynamics in the topological insulator Bi_2Te_3," Nano Lett. **12**, 3532–3536 (2012).
25. N. Kumar, B. A. Ruzicka, N. P. Butch, P. Syers, K. Kirshenbaum, J. Paglione, and H. Zhao, "Spatially resolved femtosecond pump-probe study of topological insulator Bi_2Se_3," Phys. Rev. B **83**, 235306 (2011).
26. D. Hsieh, F. Mahmood, J. W. McIver, D. R. Gardner, Y. S. Lee, and N. Gedik, "Selective probing of photoinduced charge and spin dynamics in the bulk and surface of a topological insulator," Phys. Rev. Lett. **107**, 077401 (2011).
27. C. Zhao, H. Zhang, X. Qi, Y. Chen, Z. Wang, S. Wen, and D. Tang, "Ultra-short pulse generation by a topological insulator based saturable absorber," Appl. Phys. Lett. **101**, 211106 (2012).
28. S. Lu, C. Zhao, Y. Zou, S. Chen, Y. Chen, Y. Li, H. Zhang, S. Wen, and D. Tang, "Third order nonlinear optical property of Bi_2Se_3," Opt. Express **21**, 2072–2082 (2013).
29. C. Zhao, Y. Zou, Y. Chen, Z. Wang, S. Lu, H. Zhang, S. Wen, and D. Tang, "Wavelength-tunable picosecond soliton fiber laser with topological insulator: Bi_2Se_3 as a mode locker," Opt. Express **20**, 27888–27895 (2012).
30. Z.-C. Luo, M. Liu, H. Liu, X.-W. Zheng, A.-P. Luo, C.-J. Zhao, H. Zhang, S.-C. Wen, and W.-C. Xu, "2 GHz passively harmonic mode-locked fiber laser by a microfiber-based topological insulator saturable absorber," Opt. Lett. **38**, 5212–5215 (2013).
31. J. Sotor, G. Sobon, W. Macherzynski, P. Paletko, K. Grodecki, and K. M. Abramski, "Mode-locking in Er-doped fiber laser based on mechanically exfoliated Sb_2Te_3 saturable absorber," Opt. Mater. Express **4**, 1–6 (2014).
32. J. Sotor, G. Sobon, W. Macherzynski, and K. M. Abramski, "Harmonically mode-locked Er-doped fiber laser based on a Sb_2Te_3 topological insulator saturable absorber," Laser Phys. Lett. **11**, 055102 (2014).
33. H. Liu, X.-W. Zheng, M. Liu, N. Zhao, A.-P. Luo, Z.-C. Luo, W.-C. Xu, H. Zhang, C.-J. Zhao, and S.-C. Wen, "Femtosecond pulse generation from a topological insulator mode-locked fiber laser," Opt. Express **22**, 6868–6873 (2014).
34. Y. Zhang, K. He, C. Z. Chang, C. L. Song, L. L. Wang, X. Chen, J. F. Jia, Z. Fang, X. Dai, W. Y. Shan, S. Q. Shen, Q. Niu, X. L. Qi, S. C. Zhang, X. C. Ma, and Q. K. Xue, "Crossover of the three-dimensional topological insulator Bi_2Se_3 to the two-dimensional limit," Nat. Phys. **6**, 584–588 (2010).
35. H. Peng, K. Lai, D. Kong, S. Meister, Y. Chen, X. L. Qi, S. C. Zhang, Z. X. Shen, and Y. Cui, "Aharonov–Bohm interference in topological insulator nanoribbons," Nat. Mater. **9**, 225–229 (2010).
36. D. Teweldebrhan, V. Goyal, M. Rahman, and A. A. Balandin, "Atomically-thin crystalline films and ribbons of bismuth telluride," Appl. Phys. Lett. **96**, 053107 (2010).
37. Y.-H. Lin, C.-Y. Yang, S.-F. Lin, W.-H. Tseng, Q. Bao, C.-I. Wu, and G.-R. Lin, "Soliton compression of the erbium-doped fiber laser weakly started mode-locking by nanoscale p-type Bi_2Te_3 topological insulator particles," Laser Phys. Lett. **11**, 055107 (2014).
38. M. Jung, J. Koo, P. Debnath, Y. W. Song, and J. H. Lee, "A mode-locked 1.91 μm fiber laser based on interaction between graphene oxide and evanescent field," Appl. Phys. Express **5**, 112702 (2012).
39. J. Sotor, G. Sobon, and K. M. Abramski, "Sub-130 fs mode-locked Er-doped fiber laser based on topological insulator," Opt. Express **22**, 13244–13249 (2014).
40. J. Lee, J. Koo, Y. M. Jhon, and J. H. Lee, "A femtosecond pulse erbium fiber laser incorporating a saturable absorber based on bulk-structured Bi_2Te_3 topological insulator," Opt. Express **22**, 6165–6173 (2014).
41. M. Jung, J. Lee, J. Koo, J. Park, Y.-W. Song, K. Lee, S. Lee, and J. H. Lee, "A femtosecond pulse fiber laser at 1935 nm using a bulk-structured Bi_2Te_3 topological insulator," Opt. Express **22**, 7865–7874 (2014).
42. J. Boguslawski, J. Sotor, G. Sobon, J. Tarka, J. Jagiello, W. Macherzynski, L. Lipinska, and K. M. Abramski, "Mode-locked Er-doped fiber laser based on liquid phase exfoliated Sb_2Te_3 topological insulator," Laser Phys. **24**, 105111 (2014).
43. M. Liu, N. Zhao, H. Liu, X.-W. Zheng, A.-P. Luo, Z.-C. Luo, W.-C. Xu, C.-J. Zhao, H. Zhang, and S.-C. Wen, "Dual-wavelength harmonically mode-locked fiber laser with topological insulator saturable absorber," IEEE Photon. Technol. Lett. **26**, 983–986 (2014).
44. J. Sotor, G. Sobon, K. Grodecki, and K. M. Abramski, "Mode-locked erbium-doped fiber laser based on evanescent field interaction with Sb_2Te_3 topological insulator," Appl. Phys. Lett. **104**, 251112 (2014).
45. J. Sotor, G. Sobon, J. Boguslawski, J. Tarka, K. Krzempek, and K. Abramski, "Fiber mode-locked lasers based on topological insulator saturable absorbers," in *6th EPS-QEOD EUROPHOTON Conference Digest* (European Physical Society, 2014), paper no. TuP-T1-P-10.
46. H. Liu, A.-P. Luo, F.-Z. Wang, R. Tang, M. Liu, Z.-C. Luo, W.-C. Xu, C.-J. Zhao, and H. Zhang, "Femtosecond pulse erbium-doped fiber laser by a few-layer MoS_2 saturable absorber," Opt. Lett. **39**, 4591–4594 (2014).
47. R. M. A. Lieth and J. C. J. M. Terhell, *Transition Metal Dichalcogenides* (Springer Netherlands, 1997).
48. J. A. Wilson and A. D. Yoffe, "The transition metal dichalcogenides discussion and interpretation of the observed optical, electrical and structural properties," Adv. Phys. **18**, 193–335 (1969).
49. Q. H. Wang, K. Kalantar-Zadeh, A. Kis, J. N. Coleman, and M. S. Strano, "Electronics and optoelectronics of two-dimensional transition metal dichalcogenides," Nat. Nanotechnol. **7**, 699–712 (2012).
50. M. Zhang, R. C. T. Howe, R. I. Woodward, E. J. R. Kelleher, F. Torrisi, G. Hu, S. V. Popov, J. R. Taylor, and T. Hasan, "Solution processed MoS_2-PVA composite for sub-bandgap mode-locking of a wideband tunable ultrafast Er:fiber laser," Nano Res., doi: 10.1007/s12274-014-0637-2 (to be published).

51. J. Du, Q. Wang, G. Jiang, C. Xu, C. Zhao, Y. Xiang, Y. Chen, S. Wen, and H. Zhang, "Ytterbium-doped fiber laser passively mode locked by few-layer molybdenum disulfide (MoS_2) saturable absorber functioned with evanescent field interaction," Sci. Rep. **4**, 6346 (2014).
52. M. Liu, X.-W. Zheng, Y.-L. Qi, H. Liu, A.-P. Luo, Z.-C. Luo, W.-C. Xu, C.-J. Zhao, and H. Zhang, "Microfiber-based few-layer MoS_2 saturable absorber for 2.5 GHz passively harmonic mode-locked fiber laser," Opt. Express **22**, 22841–22846 (2014).
53. R. W. Newson, J. Dean, B. Schmidt, and H. M. van Driel, "Ultrafast carrier kinetics in exfoliated graphene and thin graphite films," Opt. Express **17**, 2326–2333 (2009).
54. J. M. Dawlaty, S. Shivaraman, M. Chandrashekhar, F. Rana, and M. G. Spencer, "Measurement of ultrafast carrier dynamics in epitaxial graphene," Appl. Phys. Lett. **92**, 042116 (2008).
55. R. R. Nair, P. Blake, A. N. Grigorenko, K. S. Novoselov, T. J. Booth, T. Stauber, N. M. R. Peres, and A. K. Geim, "Fine structure constant defines visual transparency of graphene," Science **320**, 1308 (2008).
56. I. H. Baek, H. W. Lee, S. Bae, B. H. Hong, Y. H. Ahn, D.-I. Yeom, and F. Rotermund, "Efficient mode-locking of Sub-70-fs Ti:sapphire laser by graphene saturable absorber," Appl. Phys. Express **5**, 032701 (2012).
57. E. Ugolotti, A. Schmidt, V. Petrov, J. W. Kim, D.-I. Yeom, F. Rotermund, S. Bae, B. H. Hong, A. Agnesi, C. Fiebig, G. Erbert, X. Mateos, M. Aguiló, F. Diaz, and U. Griebner, "Graphene mode-locked femtosecond Yb:KLuW laser," Appl. Phys. Lett. **101**, 161112 (2012).
58. W. B. Cho, J. W. Kim, H. W. Lee, S. Bae, B. H. Hong, S. Y. Choi, I. H. Baek, K. Kim, D.-I. Yeom, and F. Rotermund, "High-quality, large-area monolayer graphene for efficient bulk laser mode-locking near 1.25 μm," Opt. Lett. **36**, 4089–4091 (2011).
59. S. D. Di Dio Cafiso, E. Ugolotti, A. Schmidt, V. Petrov, U. Griebner, A. Agnesi, W. B. Cho, B. H. Jung, F. Rotermund, S. Bae, B. H. Hong, G. Reali, and F. Pirzio, "Sub-100-fs Cr:YAG laser mode-locked by monolayer graphene saturable absorber," Opt. Lett. **38**, 1745–1747 (2013).
60. D. Popa, Z. Sun, F. Torrisi, T. Hasan, F. Wang, and A. C. Ferrari, "Sub 200 fs pulse generation from a graphene mode-locked fiber laser," Appl. Phys. Lett. **97**, 203106 (2010).
61. A. Martinez, K. Fuse, and S. Yamashita, "Mechanical exfoliation of graphene for the passive mode-locking of fiber lasers," Appl. Phys. Lett. **99**, 121107 (2011).
62. Z. Sun, D. Popa, T. Hasan, F. Torrisi, F. Wang, E. J. R. Kelleher, J. C. Travers, V. Nicolosi, and A. C. Ferrari, "A stable, wideband tunable, near transform-limited, graphene-mode-locked, ultrafast laser," Nano Res. **3**, 653–660 (2010).
63. W. Strupinski, K. Grodecki, A. Wysmolek, R. Stepniewski, T. Szkopek, P. E. Gaskell, A. Gruneis, D. Haberer, R. Bozek, J. Kupka, and J. M. Baranowski, "Graphene epitaxy by chemical vapor deposition on SiC," Nano Lett. **11**, 1786–1791 (2011).
64. Q. Bao, H. Zhang, Z. Ni, Y. Wang, L. Polavarapu, Z. Shen, Q.-H. Xu, D. Tang, and K. P. Loh, "Monolayer graphene as a saturable absorber in a mode-locked laser," Nano Res. **4**, 297–307 (2011).
65. P. L. Huang, S.-C. Lin, C.-Y. Yeh, H.-H. Kuo, S.-H. Huang, G.-R. Lin, L.-J. Li, C.-Y. Su, and W.-H. Cheng, "Stable mode-locked fiber laser based on CVD fabricated graphene saturable absorber," Opt. Express **20**, 2460–2465 (2012).
66. H. Zhang, D. Y. Tang, L. M. Zhao, Q. L. Bao, and K. P. Loh, "Large energy mode locking of an erbium-doped fiber laser with atomic layer graphene," Opt. Express **17**, 17630–17635 (2009).
67. C. C. Lee, G. Acosta, J. S. Bunch, and T. R. Schibli, "Ultra-short optical pulse generation with single-layer graphene," J. Nonlinear Opt. Phys. **19**, 767–771 (2010).
68. G. Sobon, J. Sotor, I. Pasternak, K. Grodecki, P. Paletko, W. Strupinski, Z. Jankiewicz, and K. M. Abramski, "Er-Doped fiber laser mode-locked by CVD–graphene saturable absorber," J. Lightwave Technol. **30**, 2770–2775 (2012).
69. H. Zhang, D. Y. Tang, L. M. Zhao, Q. L. Bao, K. P. Loh, B. Lin, and S. C. Tjin, "Compact graphene mode-locked wavelength-tunable erbium-doped fiber lasers: from all anomalous dispersion to all normal dispersion," Laser Phys. Lett. **7**, 591–596 (2010).
70. A. Martinez, K. Fuse, B. Xu, and S. Yamashita, "Optical deposition of graphene and carbon nanotubes in a fiber ferrule for passive mode-locked lasing," Opt. Express **18**, 23054–23061 (2010).
71. J. Tarka, G. Sobon, J. Boguslawski, J. Sotor, J. Jagiello, M. Aksienionek, L. Lipinska, M. Zdrojek, J. Judek, and K. M. Abramski, "168 fs pulse generation from graphene-chitosan mode-locked fiber laser," Opt. Mater. Express **4**, 1981–1986 (2014).
72. J. Sotor, G. Sobon, I. Pasternak, A. Krajewska, W. Strupinski, and K. M. Abramski, "Simultaneous mode-locking at 1565 nm and 1944 nm in fiber laser based on common graphene saturable absorber," Opt. Express **21**, 18994–19002 (2013).
73. J. Sotor, G. Sobon, J. Tarka, I. Pasternak, A. Krajewska, W. Strupinski, and K. M. Abramski, "Passive synchronization of erbium and thulium doped fiber mode-locked lasers enhanced by common graphene saturable absorber," Opt. Express **22**, 5536–5543 (2014).
74. W. Zeller, L. Naehle, P. Fuchs, F. Gerschuetz, L. Hildebrandt, and J. Koeth, "DFB lasers between 760 nm and 16 μm for sensing applications," Sensors **10**, 2492–2510 (2010).
75. K. Scholle, S. Lamrini, P. Koopmann, and P. Fuhrberg, "2 μm laser sources and their possible applications," in *Frontiers in Guided Wave Optics and Optoelectronics*, B. Pal, ed. (InTech, 2010).
76. M. Zhang, E. J. R. Kelleher, F. Torrisi, Z. Sun, T. Hasan, D. Popa, F. Wang, A. C. Ferrari, S. V. Popov, and J. R. Taylor, "Tm-doped fiber laser mode-locked by graphene–polymer composite," Opt. Express **20**, 25077–25084 (2012).
77. Q. Wang, T. Chen, B. Zhang, M. Li, Y. Lu, and K. P. Chen, "All-fiber passively mode-locked thulium-doped fiber ring laser using optically deposited graphene saturable absorbers," Appl. Phys. Lett. **102**, 131117 (2013).
78. G. Sobon, J. Sotor, I. Pasternak, A. Krajewska, W. Strupinski, and K. M. Abramski, "Thulium-doped all-fiber laser mode-locked by CVD-graphene/PMMA saturable absorber," Opt. Express **21**, 12797–12802 (2013).